



Multi-Parameter Analysis and Operating Cost Optimization for NO Removal using Active Coke

Journal:	<i>Science Progress</i>
Manuscript ID	SCI-25-1477
Manuscript Type:	Original Research Article
Date Submitted by the Author:	02-Jul-2025
Complete List of Authors:	Liu, Wen; North China Electric Power University Liu, Huawei; North China Electric Power University, Cheng, Wei liang; North China Electric Power University
Keywords:	NO removal, Active coke, Machine learning, Genetic algorithm optimization, Economic optimization
Abstract:	<p>Currently, the removal of nitrogen oxides (NO_x) is one of the most critical environmental challenges. Notably, active coke denitrification has emerged as an effective method for NO_x removal. However, research on the effect of operating parameters and their optimization on the performance and cost-efficiency of NO_x removal remains limited. Therefore, this study designs a simulation model using COMSOL software to analyze the denitrification process in a pipe packed with active coke particles. The effects of key operating parameters on NO_x removal efficiency are investigated. Additionally, an optimization approach is introduced. A neural network-based predictive model is developed and trained using a large dataset from simulation results. A genetic algorithm is then applied to minimize operating costs and maintain effective denitrification. Key parameters, including pipe diameter, temperature, flow velocity, pipe length, and NO concentration in the inlet flue gas, are optimized. The results reveal that temperature, flow velocity, pipe length, and inlet NO concentration significantly influence the efficiency of active coke denitrification. However, pipe diameter has minimal impact on denitrification performance but directly determines the volume of flue gas processed. Moreover, the optimization of temperature, flow velocity, and pipe length significantly reduces operating costs and ensures compliance with denitrification efficiency standards.</p>

SCHOLARONE™
Manuscripts

1
2
3
4
5
6
7
8
9
10
11
12
13
14
15
16
17
18
19
20
21
22
23
24
25
26
27
28
29
30
31
32
33
34
35
36
37
38
39
40
41
42
43
44
45
46
47
48
49
50
51
52
53
54
55
56
57
58
59
60

Multi-Parameter Analysis and Operating Cost Optimization for NO Removal using Active Coke

Wen Liu, Huawei Liu*, Weiliang Cheng

Key Laboratory of Power Station Energy Transfer Conversion and System of MOE, School of Energy Power and Mechanical Engineering, North China Electric Power University, Beijing 102206, PR China

*Corresponding author. E-mail address: liuhw@ncepu.edu.cn

Abstract:

Currently, the removal of nitrogen oxides (NO_x) is one of the most critical environmental challenges. Notably, active coke denitrification has emerged as an effective method for NO_x removal. However, research on the effect of operating parameters and their optimization on the performance and cost-efficiency of NO_x removal remains limited. Therefore, this study designs a simulation model using COMSOL software to analyze the denitrification process in a pipe packed with active coke particles. The effects of key operating parameters on NO_x removal efficiency are investigated. Additionally, an optimization approach is introduced. A neural network-based predictive model is developed and trained using a large dataset from simulation results. A genetic algorithm is then applied to minimize operating costs and maintain effective denitrification. Key parameters, including pipe diameter, temperature, flow velocity, pipe length, and NO concentration in the inlet flue gas, are optimized. The results reveal that temperature, flow velocity, pipe length, and inlet NO concentration significantly influence the efficiency of active coke denitrification. However, pipe diameter has minimal impact on denitrification performance but directly determines the volume of flue gas processed. Moreover, the optimization of temperature,

22 flow velocity, and pipe length significantly reduces operating costs and ensures compliance with
23 denitrification efficiency standards.

24 **Keywords: NO removal; Active coke; Machine learning; Genetic algorithm optimization;**
25 **Economic optimization.**

26 **Highlights**

- 27 1. NO removal using active coke particles was investigated via numerical simulations.
- 28 2. A neural network model was developed to predict denitrification efficiency.
- 29 3. Key operating parameters were optimized to enhance denitrification performance.
- 30 4. The optimization significantly reduced costs and maintained effective denitrification.

1
2
3
4
5
6
7
8
9
10
11
12
13
14
15
16
17
18
19
20
21
22
23
24
25
26
27
28
29
30
31
32
33
34
35
36
37
38
39
40
41
42
43
44
45
46
47
48
49
50
51
52
53
54
55
56
57
58
59
60

31 **1. Introduction**

32 Nitrogen oxides (NO_x) are one of the major pollutants in industrial emissions [1]-[4]. These oxides
33 are chemically diverse [5]-[7] and pose significant risks to both environment and human health [8].
34 Therefore, the control and reduction of NO_x emissions remain a key challenge in environmental
35 engineering and are crucial for achieving clean, sustainable development. Currently, NO_x control
36 techniques include selective catalytic reduction (SCR) [9], selective non-catalytic reduction (SNCR),
37 alkaline absorption, acid absorption, O₃ oxidative absorption, plasma activation [10], active coke
38 denitrification (ACD) [11], carbothermal reduction [12], low-temperature plasma technology [13],
39 biological denitrification [14], and photocatalytic oxidation [15].

40 In industrial NO_x control, SCR, SNCR, and ACD are the main techniques adopted. SCR is a well-
41 established flue gas denitrification method in which ammonia or urea solution is injected into the flue
42 gas in the presence of a catalyst. This process facilitates the reduction of NO_x into nitrogen and water.
43 SCR achieves high denitrification efficiency (often exceeding 90%) and effectively operates at low
44 temperatures (typically 250°C–400°C). SCR systems exhibit long catalyst lifespans (up to 2–3 years)
45 and produce minimal toxic byproducts. However, SCR faces certain limitations, including high catalyst
46 costs, significant operating and maintenance expenses, and the need for additional equipment to supply
47 ammonia or urea solutions. Moreover, the presence of pollutants can impair catalyst performance in SCR,
48 leading to variability in denitrification efficiency. In contrast, SNCR involves the direct injection of
49 ammonia or urea solution into a high-temperature zone. The injected solution reacts with NO_x in the flue
50 gas, which reduces NO_x to nitrogen and water. SNCR has low equipment and operating costs, requires
51 no catalyst, and features simple operation. SNCR is easy to implement and maintain, making it suitable
52 for high-temperature flue gas environments in coal-fired power plants. However, SNCR exhibits lower

denitrification efficiency (typically 30%–60%) than SCR. Additionally, SNCR requires stable high flue gas temperatures (typically 850 to 1100°C) and may produce NO_x during operation, potentially causing air pollution [16]. These limitations hinder the broader application of SNCR. ACD is an integrated flue gas purification technique that combines adsorption and catalytic properties to remove SO₂ and NO_x. ACD enables low-temperature denitrification, which significantly reduces energy consumption. Therefore, ACD is increasingly recognized as a promising technique for NO removal [17].

With the widespread application of the ACD technique in industrial flue gas purification, its economic performance has become a key research focus. Yang et al. [18] conducted a comparative study of two efficient NO_x control methods (ACD and SCR). A cost-benefit analysis model was developed to assess the economic viability of typical systems using these techniques. The study provides insights into the specific effects of key factors, such as operating hours and material costs, on overall performance. Brozinčević et al. [19] focused on reducing costs in biological denitrification using conventional and alternative carbon sources. The study systematically investigated the use of different organic carbon sources (e.g., wood chips and corn cobs) in the denitrification process and comparatively analyzed their cost-effectiveness. Yang [20] estimated the initial investment for flue gas denitrification techniques using active coke and limestone-gypsum. Moreover, operating costs were calculated based on raw material and product prices in China. The economic performance of active coke and limestone-gypsum denitrification was compared and analyzed across different usage periods. Wu et al. [21] investigated cost reduction and resource recovery strategies through cross-flow adsorption of active coke, optimization of waste heat recovery, regeneration gas treatment, and high-temperature regeneration techniques. These methods contributed to the reduction of ACD costs. Liu [22] designed equipment to further reduce ACD costs by integrating resource recycling, automated control, and optimized adsorbent materials into a streamlined

1
2
3
4
5
6
7
8
9
10
11
12
13
14
15
16
17
18
19
20
21
22
23
24
25
26
27
28
29
30
31
32
33
34
35
36
37
38
39
40
41
42
43
44
45
46
47
48
49
50
51
52
53
54
55
56
57
58
59
60

75 system. Chen et al. [23] simplified the desulfurization and denitrification process by combining dedusting,
76 cooling, ammonia injection, and adsorption regeneration functions into a single unit, thereby reducing
77 equipment complexity and cost.

78 However, current studies have not sufficiently explored the complex interactions among operating
79 parameters such as temperature, flow velocity, pipe length, and inlet conditions. Further research is
80 needed to examine the effects of these parameters on denitrification performance and operating costs, as
81 they are critical for optimizing the ACD technique and maximizing its economic benefits.

82 In recent years, numerical simulations and machine learning techniques have proven highly effective
83 in addressing complex optimization challenges in denitrification processes. For example, a genetic
84 algorithm-optimized Back Propagation neural network was used to design catalyst volume in an SCR
85 system. The model, trained on operational data under different operating conditions, accurately predicted
86 the required catalyst volume for efficient SCR operation [24]. Additionally, neural network-based
87 predictive control methods have been applied to monitor and regulate NOx emissions in power plant tail
88 gas. Ammonia injection was regulated through model calibration and predictive control strategies to meet
89 emission standards, reduce ammonia consumption, and minimize ammonia slip. These measures
90 improved the economic efficiency of the NOx control system [25].

91 Genetic algorithms have been used to optimize operating parameters in SCR systems. For example, a
92 combination of neural networks and genetic algorithms was used to predict the control structure and
93 optimize catalyst volume for ammonia injection control. Simulation results revealed that this combined
94 approach can reduce denitrification costs, adapt to a wide range of boiler conditions, and ensure
95 compliance with emission standards [26]. Additionally, ultra-low-temperature (<150°C) SCR
96 denitrification technology has emerged as a key research focus. Although China has developed SCR

1
2
3 97 systems and corresponding catalysts with good performance in the 180°C–420°C range, further
4
5
6 98 advancements are needed to ensure effective operation at lower temperatures. Ultra-low-temperature
7
8
9 99 SCR denitrification systems can be installed downstream of the dust remover and desulfurization tower
10
11 100 owing to their simpler flue gas composition, lower energy consumption, and reduced retrofit costs [27].
12
13
14 101 Therefore, the low-temperature operation of ACD provides a distinct advantage.

15
16 102 Overall, the combined use of ACD technology, numerical simulation, machine learning, and genetic
17
18
19 103 algorithms in the denitrification process provides innovative approaches for achieving clean and
20
21
22 104 sustainable denitrification. These techniques enhance denitrification efficiency, reduce operating costs,
23
24
25 105 and adapt to the evolving demands of industrial flue gas purification. Future research should further
26
27 106 investigate the integrated application of these methods to maximize economic benefits.

28
29 107 Therefore, this paper comprehensively investigates key operating parameters in the ACD process. First,
30
31
32 108 a denitrification model is developed using COMSOL software to simulate flue gas flow through a pipe
33
34
35 109 filled with active coke. The effects of key operating parameters on ACD system performance are
36
37
38 110 analyzed. The resulting large dataset is used to train a neural network predictive model. Moreover, an
39
40
41 111 economic assessment model is constructed to evaluate the operating costs of the denitrification process.
42
43
44 112 Finally, the predictive model, economic assessment model, and genetic algorithm are integrated to
45
46
47 113 optimize the configuration of operating parameters and maintain high denitrification efficiency.

48 114 The paper is structured as follows: First, the COMSOL model, neural network predictive model,
49
50
51 115 genetic algorithm, and economic assessment model are introduced. Subsequently, the effects of key
52
53
54 116 operating parameters—pipe diameter, temperature, flow velocity, pipe length, and inlet NO
55
56
57 117 concentration—on denitrification performance are analyzed. The neural network predictive model is
58
59
60 118 developed and validated. Optimal operating parameters are identified under different conditions using a

1
2
3
4
5
6
7
8
9
10
11
12
13
14
15
16
17
18
19
20
21
22
23
24
25
26
27
28
29
30
31
32
33
34
35
36
37
38
39
40
41
42
43
44
45
46
47
48
49
50
51
52
53
54
55
56
57
58
59
60

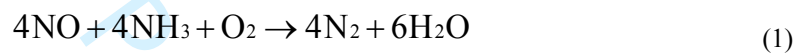
119 cost-minimization objective, ensuring compliance with NO emission limits in the outlet flue gas. Finally,
120 the main conclusions of the study are summarized.

For Peer Review

2. Methodology

2.1 ACD simulation

In the ACD simulation, only NO is considered the target product. NO in the flue gas is first adsorbed onto the surface functional groups of the active coke. In the presence of active coke as a catalyst, NO undergoes a redox reaction with ammonia and oxygen, forming nitrogen and water. The oxygen required for this reaction is supplied by the flue gas. Before the flue gas enters the active coke reactor, ammonia is injected into the flue gas stream to ensure thorough mixing of the reactants [30]. In this study, the ACD process is numerically simulated using COMSOL Multiphysics software. The chemical reaction [29] for NO removal is as follows:



A pipe packed with active coke serves as the reactor. The pipe (**Fig. 1**) has a standard nominal diameter D and a length L . The flue gas, containing NO and mixed with ammonia, flows into the pipe at the left end and exits at the right end.

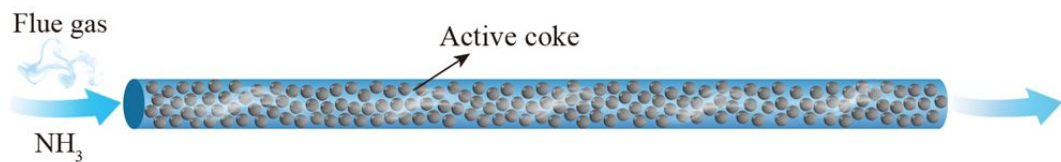


Fig. 1. Schematic of the denitrification pipe.

The denitrification pipe (**Fig. 1**) is packed with spherical active coke particles, with a radius r of 4.5 mm [28]. These particles are randomly arranged using a distribution algorithm that assigns coordinates (x, y) to form a packed bed of active coke (**Fig. 2**).

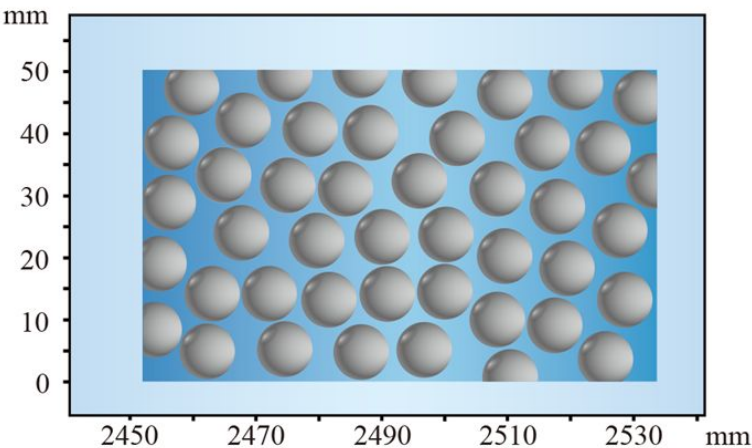


Fig. 2. Schematic of the randomly distributed active coke bed.

During the random placement of active coke particles, ensuring spatial separation and complete confinement of the particles within the reactor boundaries is crucial. The specific constraints are as follows:

$$\sqrt{(x_i - x_j)^2 + (y_i - y_j)^2} > 2r, r < x < L - r, r < y < D - r. \tag{2}$$

A two-dimensional (2D) model is developed in COMSOL software using the free and porous media flow, dilute species transport, and multiphysics coupling modules. In this model, free and porous media flow is analyzed under steady-state conditions. The dilute species transport and multiphysics coupling are simulated through transient analysis [31].

Simulations are conducted to investigate the effects of inlet flow velocity, inlet NO concentration, temperature [32], pipe diameter [33], and pipe length on denitrification performance. The specific parameter ranges are shown in **Table 1**.

Table 1. Simulation parameter ranges.

Temperature (°C)	Pipe diameter (mm)	Pipe length (mm)	Inlet concentration (mol/m ³)	Inlet flow velocity (m/s)
110~150	50 80	800~3000	0.02~0.04	3~5

After simulation, the outlet NO concentrations are obtained from data extracted along the centerline defined in the 2D model [31] (**Fig. 3**).

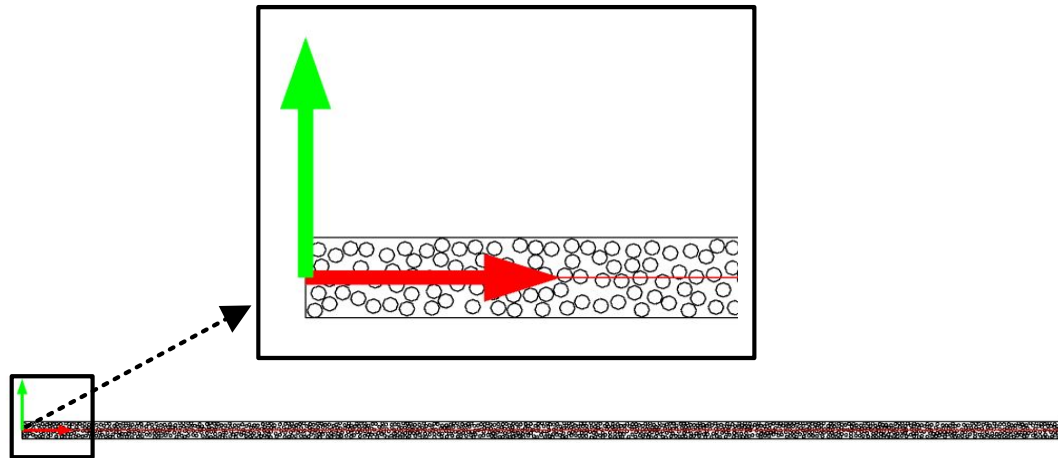


Fig. 3. Schematic of the centerline path.

The centerline is positioned between the midpoints of the inlet and outlet of the denitrification pipe and is aligned with the pipe axis (**Fig. 3**). This alignment is oriented in the direction of flue gas flow, enabling detailed observation of NO concentration distribution. Therefore, variations in NO concentration during denitrification can be further analyzed.

2.2 Neural network models

The MATLAB Neural Network Toolbox is widely used by researchers and engineers to develop advanced models. The toolbox provides a comprehensive set of modules, including feedforward neural networks, radial basis function networks, and deep neural networks, making it suitable for various applications [34]. Notably, MATLAB neural network fitting models are effective for modeling nonlinear and multidimensional input–output systems [35]. Additionally, MATLAB Deep Learning Toolbox extends its functionality to support the efficient construction of advanced neural network architectures, such as convolutional neural networks and recurrent neural networks. These architectures provide strong technical support for addressing complex issues [36].

In this study, a predictive model for outlet NO concentration was developed using the MATLAB Neural Network Fitting Toolbox. A large amount of training data was generated from simulations conducted in COMSOL software. The model (**Fig. 4**) utilizes a feedforward neural network architecture trained using the backpropagation algorithm. To improve prediction accuracy, the number of hidden layers and neurons in the network was carefully optimized. During training, the dataset was split into three subsets: 70% for training,

1
2
3
4
5
6
7
8
9
10
11
12
13
14
15
16
17
18
19
20
21
22
23
24
25
26
27
28
29
30
31
32
33
34
35
36
37
38
39
40
41
42
43
44
45
46
47
48
49
50
51
52
53
54
55
56
57
58
59
60

15% for validation, and 15% for testing. This data partitioning ensured the generalization ability and predictive performance of the model.

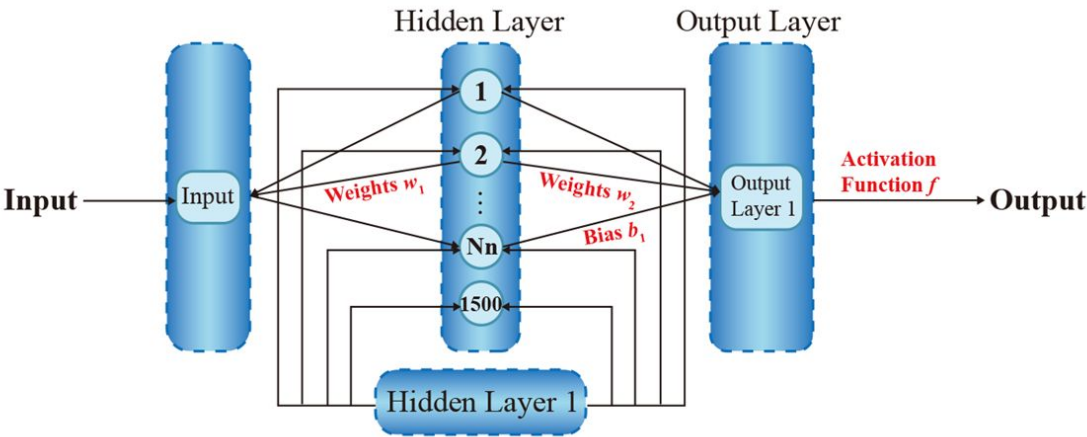


Fig. 4. Schematic of the neural network model.

2.3 Genetic algorithm optimization

The MATLAB Genetic Algorithm Toolbox is widely used in optimization research. The toolbox provides core genetic algorithm operations (such as population initialization, selection, crossover, and mutation) and supports custom fitness function design for adaptable optimization [37]. Owing to its flexibility, the toolbox is effective for solving complex, high-dimensional, nonlinear optimization tasks [38]. MATLAB genetic algorithms are recognized for their global optimization capability, scalability, and computational efficiency [39]. These algorithms have been widely used in engineering optimization [40], chemical process optimization [41], computer simulation and modeling [42]. With continuous advancements in computational technologies and algorithm theory, genetic algorithms exhibit strong potential for addressing complex optimization challenges, particularly in machine learning, data mining, and big data analysis [43].

In this study, the outlet NO concentration is limited to a maximum of 50 mg/m³ (equivalent to 0.00167 mol/m³ denoted as C_{std}) according to the national emission standard [44]. Given pipe diameters and inlet NO concentrations, a MATLAB-trained neural network model optimized with a genetic algorithm is used to determine the optimal temperature, inlet flow velocity, and pipe length. Additionally, the operating parameters are optimized to ensure a cost-effective ACD process. Fig. 5 shows the genetic algorithm optimization process through an intuitive flowchart, which outlines the key steps to achieve this goal.

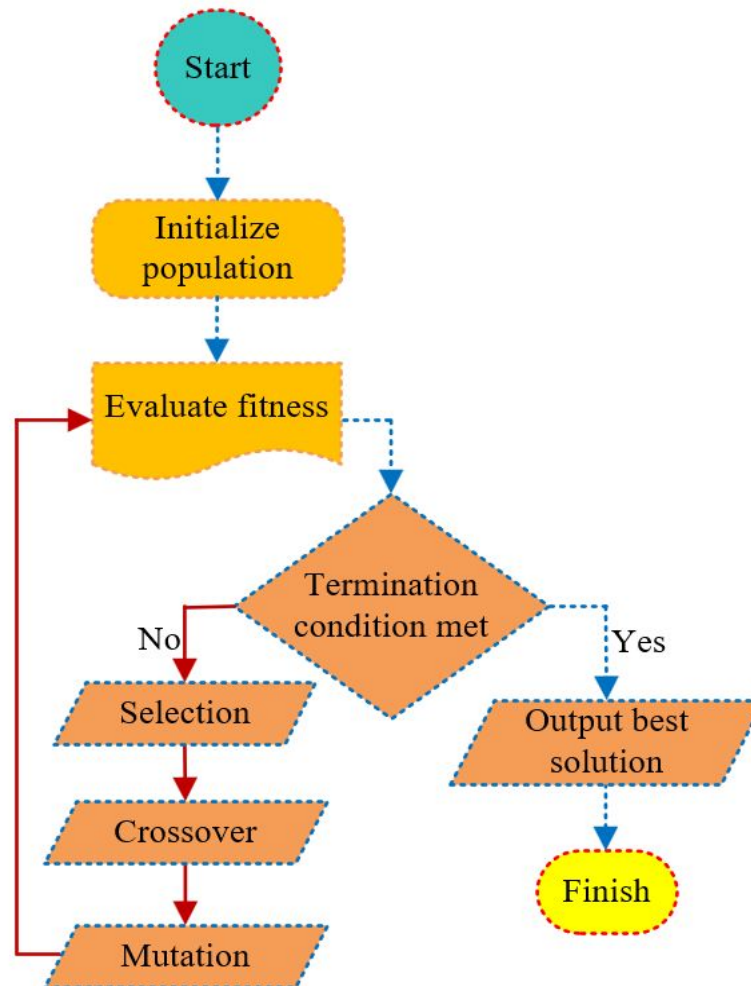


Fig. 5. Overview of the genetic algorithm optimization process.

The operating parameters of the denitrification system were optimized using a genetic algorithm to minimize the hourly operating cost (P) and the cost per unit mass of processed flue gas P' . The optimization variables include the field temperature (T), inlet flow velocity (v), and pipe length (L). The objective function and constraints are presented below:

1) Hourly cost of active coke supply (P_1)

$$P_1 = A \cdot L \cdot p_{FeMn} \cdot r_{FeMn}, \quad (3)$$

where A represents the cross-sectional area of the pipe (m^2), L denotes the pipe length (m), p_{Fe-Mn} indicates the unit price of iron–manganese-catalyzed active coke (24000 CNY/ m^3), and r_{FeMn} signifies the hourly replenishment rate (%), which is set at 10% in this study. Iron–manganese-catalyzed active coke is selected for its favorable cost-effectiveness.

206 2) Hourly heating cost of active coke P_{21}

$$207 \quad P_{21} = \frac{h \cdot S \cdot (T - T_1) \cdot P_{\text{elec}}}{1000 \cdot \eta_1} + \frac{C_{FeMn} \cdot M_{FeMn, sup} \cdot (T - T_1) \cdot P_{\text{elec}}}{3600 \cdot \eta_1}, \quad (4)$$

208 where h denotes the heat transfer coefficient between the pipe reactor and the environment ($\text{W}/(\text{m}^2 \cdot \text{K})$), which
 209 is set to $18 \text{ W}/(\text{m}^2 \cdot \text{K})$ for a 50 mm diameter pipe and $16.5 \text{ W}/(\text{m}^2 \cdot \text{K})$ for an 80 mm diameter pipe. S indicates
 210 the surface area of the pipe (m^2), P_{elec} signifies the industrial electricity price (0.725 CNY/kWh), T represents
 211 the operating temperature ($^{\circ}\text{C}$), and T_1 indicates the ambient temperature (25°C). η_1 denotes the efficiency of
 212 electromagnetic heating (95%). C_{FeMn} represents the specific heat capacity of the active coke ($1.1 \text{ kJ}/(\text{kg} \cdot \text{K})$),
 213 $M_{FeMn, sup}$ denotes the mass of active coke replenished per hour (kg), and ρ_{FeMn} signifies the density of the
 214 active coke ($800 \text{ kg}/\text{m}^3$). The hourly replenished mass is calculated as: $M_{FeMn, sup} = \rho_{FeMn} \cdot A \cdot L \cdot r_{FeMn}$.

215 3) Hourly heating cost of flue gas P_{22}

$$216 \quad P_{22} = \frac{v \cdot A \cdot \rho_{Air} \cdot C_{Air} \cdot (T - T_1) \cdot P_{\text{elec}}}{\eta_1}, \quad (5)$$

217 where v denotes the flow velocity of the flue gas (m/s), ρ_{Air} , represents the density of the flue gas (1.293
 218 kg/m^3), and C_{Air} represents the specific heat capacity of the flue gas ($1.006 \text{ kJ}/(\text{kg} \cdot \text{K})$).

219 4) Hourly operating cost of the fan P_3

$$220 \quad P_3 = \frac{v \cdot A \cdot P_{\text{fan}} \cdot P_{\text{elec}}}{\eta_2}, \quad (6)$$

221 where P_{fan} denotes the fan wind pressure (15 kPa), and η_2 indicates the fan efficiency (80%).

222 5) Penalty cost for exceeding emission standards P_4

$$223 \quad P_4 = \max(C_{out} - C_{std}, 0) \cdot (v \cdot 3600) \cdot A \cdot M_{NO} \cdot P_{\text{fine}}, \quad (7)$$

224 where \max denotes the maximum value function, ensuring the penalty remains non-negative, C_{out} represents
 225 the NO concentration in the flue gas after denitrification (mol/m^3), and C_{std} denotes the NO emission standard
 226 (mol/m^3). M_{NO} indicates the molecular weight of NO, and P_{fine} signifies the penalty cost per mass of NO. In
 227 this study, P_{fine} is set to $10,000 \text{ CNY/kg}$ to highlight the economic impact of exceeding emission limits and
 228 promote compliance with environmental standards.

229 6) Total hourly operating cost P

$$230 \quad P = P_1 + P_{21} + P_{22} + P_3 + P_4. \quad (8)$$

231 7) Cost per unit mass of processed flue gas P'

232
$$P' = \frac{P}{v \cdot 3600 \cdot A \cdot \rho_{Air}} . \quad (9)$$

For Peer Review

3. COMSOL simulation and neural network training

3.1 Validation of COMSOL simulation

To confirm the reliability of the COMSOL simulation model, a fixed-bed reactor model was developed (Fig. 7) to replicate the experimental setup in Fig. 6 [45]. In the simulation, spherical active coke particles with a diameter of 10 mm were packed into a cylindrical pipe. Although the reference study used columnar active coke particles, their height was not specified. Therefore, spherical particles of equivalent diameters (10 mm) were used to ensure consistency. The geometric configuration and boundary conditions of the model were defined as follows: the fixed bed had a height of 50 cm and a diameter of 2 cm, and the reaction was conducted at 130°C. A simulated flue gas mixture containing NH₃, NO_x, O₂, and H₂O entered from the top of the reactor and exited from the bottom. The gas flow rate was maintained at 2 L/min, and the reaction proceeded continuously for 1 h.

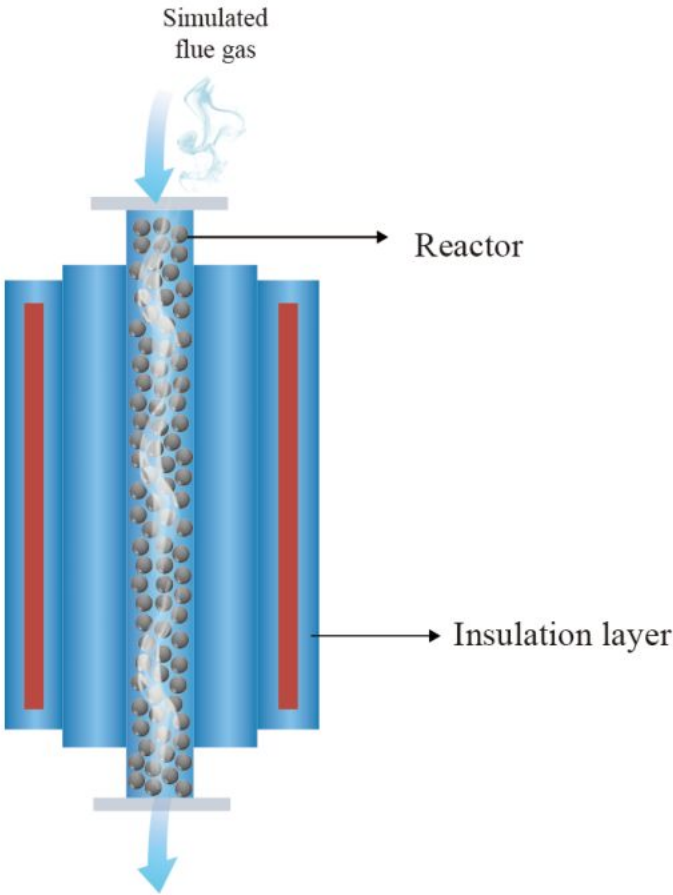


Fig. 6. Schematic of the experimental setup [45].

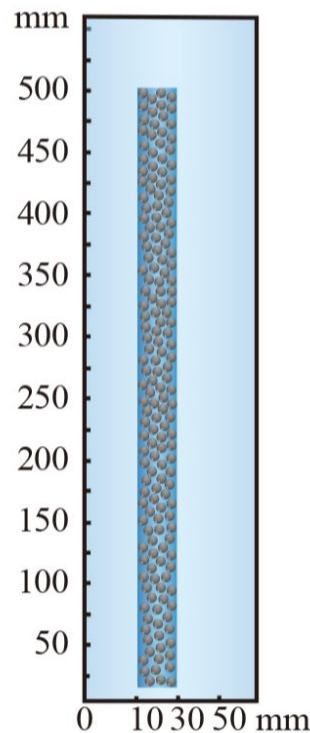
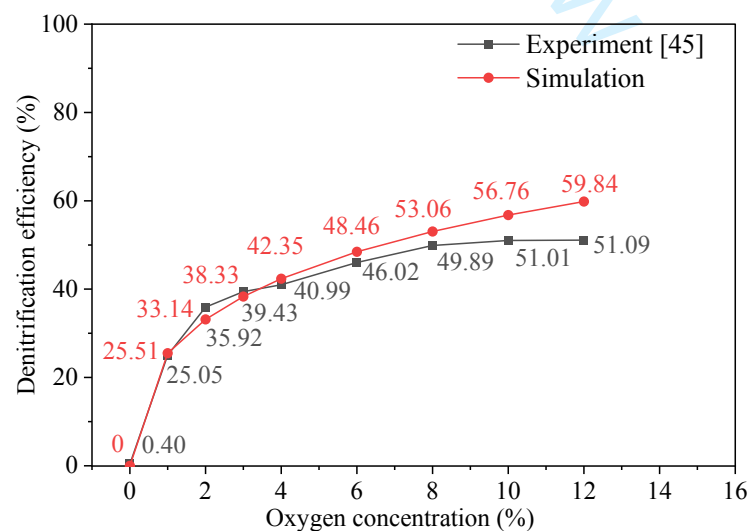


Fig. 7. Geometric model of the fixed-bed reactor.

To comprehensively validate the reliability of the COMSOL simulation model, this study examined two key operating conditions: oxygen concentrations (0%, 1%, 2%, 3%, 4%, 6%, 8%, 10%, and 12%) and volumetric flow rates (1, 2, and 4 L/min). Simulation results were directly compared with experimental data to assess accuracy. **Fig. 8** presents the denitrification efficiency of active coke across the different oxygen concentrations, while **Table 2** summarizes the corresponding results for varying volumetric flow rates.



1
2
3
4
5
6
7
8
9
10
11
12
13
14
15
16
17
18
19
20
21
22
23
24
25
26
27
28
29
30
31
32
33
34
35
36
37
38
39
40
41
42
43
44
45
46
47
48
49
50
51
52
53
54
55
56
57
58
59
60

Fig. 8. Denitrification efficiency of active coke at different oxygen concentrations.

Table 2. Denitrification efficiency of active coke at different volumetric flow rates.

Volumetric flow rates (L/min)	Denitrification efficiency (%)	
	Experiment	Simulation
1	81.32%	76.10%
2	46.62%	47.14%
4	28.13%	26.27%

The simulation results are consistent with the experimental data (**Fig. 8** and **Table 2**). This indicates that the developed denitrification model can reliably predict the denitrification efficiency of active coke. This consistency confirms the reliability and suitability of the model for further in-depth research.

3.2 Analysis of simulation results

Simulations were conducted using the established model. **Fig. 9** shows the simulated distribution of NO concentration in the pipe during denitrification. In the simulation, the pipe has a diameter of 50 mm and a length of 3000 mm. The inlet flue gas has a flow velocity of 3 m/s with an initial NO concentration of 0.02 mol/m³. The temperature within the pipe is uniformly maintained at 120°C. As the flue gas flows through the pipe, the NO concentration gradually decreases along the flow direction owing to the catalytic activity of active coke treated with an iron–manganese catalyst. Therefore, the NO concentration in the outlet flue gas is significantly lower than that in the inlet flue gas, indicating effective NO removal. The outlet NO concentration is 0.000766 mol/m³, which is below the emission standard of 0.00167 mol/m³. Despite the effectiveness of the denitrification process, its performance is influenced by several operating parameters. Therefore, the effects of pipe diameter, temperature, flow velocity, pipe length, and the inlet NO concentration on the outlet NO concentration were further analyzed.

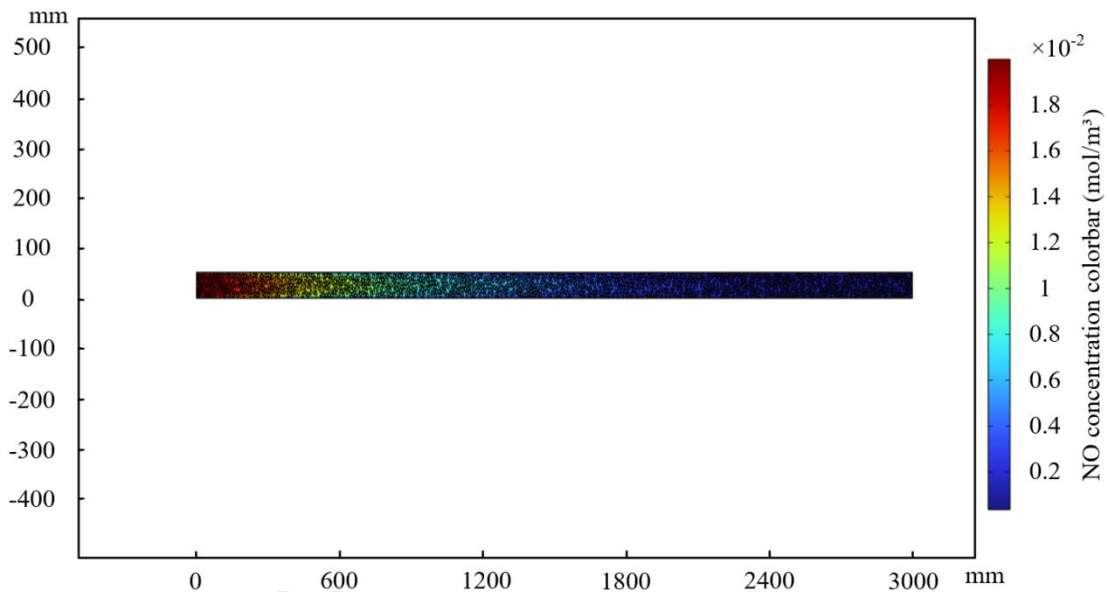


Fig. 9. Simulated distribution of NO concentration.

3.2.1 Effect of pipe diameter on the outlet NO concentration

According to standard pipe production specifications, two pipe diameters (50 and 80 mm) were selected for analysis. Simulations were performed at a temperature of 120°C, with an inlet NO concentration of 0.02 mol/m³, a pipe length of 1100 mm, and a flow velocity of 3 m/s. The outlet NO concentration was determined from the endpoint value along the pipe centerline. Simulation results for both pipe diameters are shown in Table 3. As all other conditions are held constant, increasing the pipe diameter does not significantly affect the outlet NO concentration but results in a larger total flue gas volume. If the total flue gas volume remains constant, a large pipe diameter reduces the flow velocity, which increases the residence time and results in a lower outlet NO concentration (Table 3). Moreover, pipe diameter directly affects the volume of active coke required and the associated energy consumption. Therefore, comprehensive optimization of different nominal diameters will be conducted.

Table 3. Effect of pipe diameter on the outlet NO concentration.

Temperature (°C)	Pipe diameter (mm)	Pipe length (mm)	Inlet concentration (mol/m ³)	Flow velocity (m/s)	Amount of flue gas processed per hour (m ³ /s)	Outlet concentration (mol/m ³)
120	50	1100	0.02	3	0.0059	0.007054
	80			3	0.0151	0.006972
	80			1.17	0.0059	0.000882

3.2.2 Effect of temperature on the outlet NO concentration

The effect of temperature on the outlet NO concentration was investigated through simulations. The model parameters included a pipe diameter of 50 mm, an inlet NO concentration of 0.02 mol/m³, a pipe length of 1100 mm, and a flow velocity of 3 m/s. Simulations were conducted at 110°C, 115°C, 120°C, 125°C, 135°C, and 150°C. The results are shown in Fig. 10.

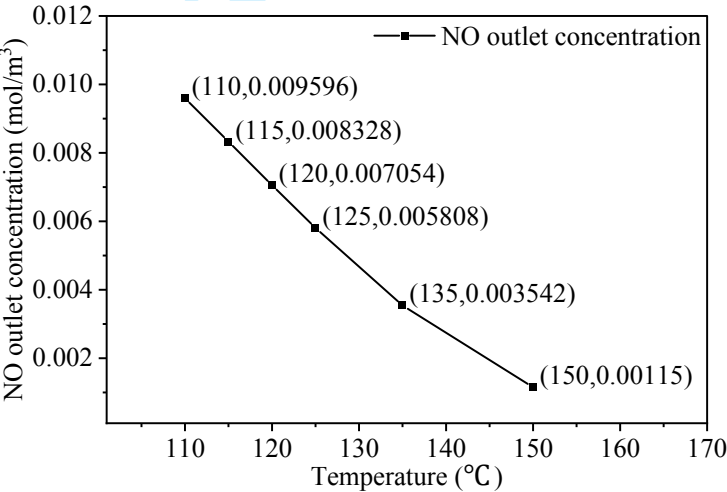


Fig. 10. Effect of temperature on the outlet NO concentration.

The data in Fig. 10 indicate a significant decrease in the outlet NO concentration with increasing temperature. In the ACD process, this trend is mainly attributed to the enhanced surface activity of active coke at higher temperatures. Higher temperatures promote the development of pore structure and increase the activity of surface active sites, thereby accelerating NO adsorption and reduction. Additionally, increased temperatures enhance the denitrification reaction kinetics, leading to more efficient NO conversion. Moreover, higher temperatures facilitate more effective contact between the reductant and NO molecules, which improves gas diffusion and further promotes the reaction. Consequently, the denitrification

performance of active coke is significantly enhanced with increasing temperature, reflected by the continuous decrease in outlet NO concentrations.

3.2.3 Effect of flow velocity on the outlet NO concentration

The effect of flow velocity on the outlet NO concentration was analyzed using a pipe diameter of 50 mm, an inlet NO concentration of 0.02 mol/m³, a temperature of 120°C, and a pipe length of 1100 mm. **Fig. 11** presents the simulation results at flow velocities of 3, 3.4, 3.8, 4.2, 4.6, and 5 m/s.

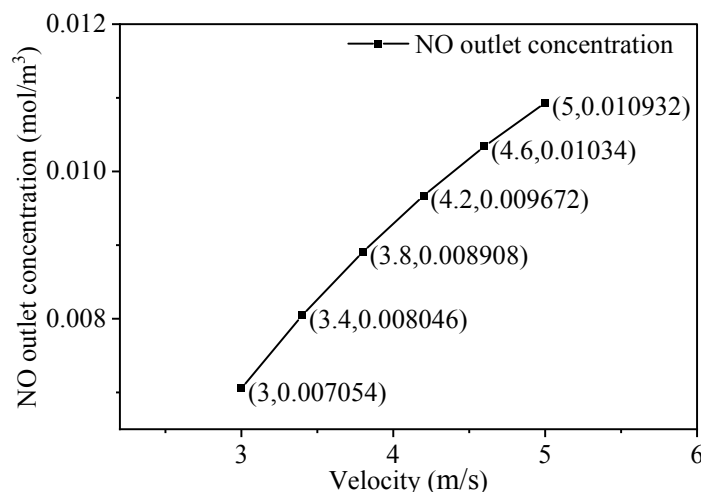


Fig. 11. Effect of flow velocity on the outlet NO concentration.

The results (**Fig. 11**) indicate the significant effect of flow velocity on the outlet NO concentration. Specifically, as the flow velocity increases, the outlet NO concentration increases. This trend can be attributed to several key factors. First, higher flow velocity shortens the residence time of the flue gas in the pipe, which reduces the likelihood of NO molecules interacting with the active coke surface for reduction reactions. Second, increased flow velocity reduces the diffusion efficiency of gas molecules, which limits the penetration of both the reductant and NO into the microporous structure of the active coke. This limitation hinders the effective utilization of reactive sites. Consequently, higher flow velocities lead to reduced overall denitrification efficiency, reflected by the increasing outlet NO concentration.

3.2.4 Effect of pipe length on the outlet NO concentration

The effect of pipe length on the outlet NO concentration was analyzed using a pipe diameter of 50 mm, an inlet NO concentration of 0.02 mol/m³, a temperature of 120°C, and a flow velocity of 3 m/s. Simulations were performed for pipe lengths of 800, 1100, 1400, 1700, 2000, and 2300 mm. The results are presented in **Fig. 12**.

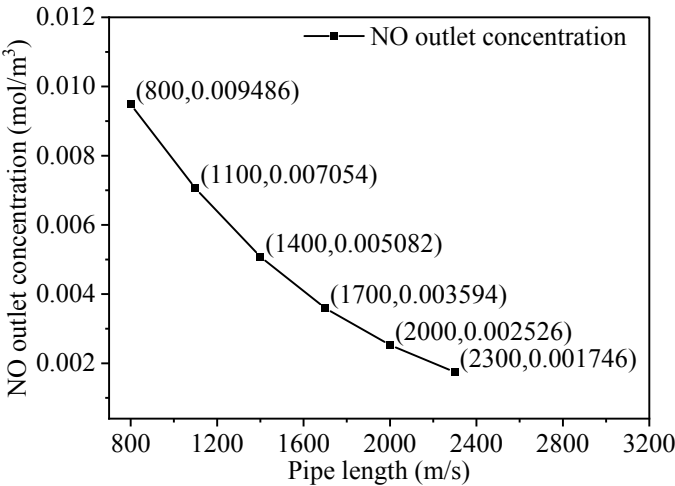


Fig. 12. Effect of pipe length on the outlet NO concentration.

The trend in **Fig. 12** indicates a decrease in the outlet NO concentration with increasing pipe length. This behavior can be attributed to several key factors. First, a longer pipe length increases the residence time of the flue gas. This provides more time for reactions between NO molecules and active coke, which enhances conversion efficiency. Second, a greater pipe length expands the contact area between the flue gas and the active coke and increases the number of available reactive sites, which promotes both physical adsorption and chemical reduction of NO. Additionally, a longer pipe facilitates homogeneous mixing of the reductant and NO molecules, further enhancing reaction kinetics. Consequently, the increased pipe length significantly improves denitrification efficiency, as indicated by the lower outlet NO concentrations.

3.2.5 Effect of inlet NO concentration on the outlet NO concentration

The effect of inlet NO concentration on the outlet NO concentration was investigated using a pipe diameter, temperature, flow velocity, and pipe length set at 50 mm, 120°C, 3 m/s, and 1100 mm, respectively. The simulation results are shown in **Table 4**. As the inlet NO concentration increases, the outlet NO concentration increases, reflecting the larger amount of NO requiring treatment.

Table 4. Effect of inlet NO concentration on the outlet NO concentration.

Temperature (°C)	Pipe diameter (mm)	Pipe length (mm)	Inlet concentration (mol/m ³)	Flow velocity (m/s)	Outlet concentration (mol/m ³)
120	50	1100	0.02	3	0.007054
			0.03		0.011205
			0.04		0.015524

These findings indicate that all five parameters significantly influence denitrification performance and are interdependent. Moreover, these factors directly affect operating costs. Because pipe diameter is limited by production standards and the NO concentration in the flue gas is a fixed input in practical applications, a simultaneous optimization of temperature, flow velocity, and pipe length was conducted.

3.3 MATLAB neural network model training and performance evaluation

Numerous simulations were conducted using COMSOL software based on the parameter ranges provided in **Table 1**. The resulting data, including operating parameters and NO concentrations after denitrification, were used to train a neural network predictive model in MATLAB. The model was developed to predict the NO concentration after denitrification using key operating parameters (temperature, pipe diameter, pipe length, inlet concentration, and flow velocity) as input variables. To comprehensively assess model predictive accuracy, its outputs were compared with the COMSOL simulation data. **Fig. 13** shows the evaluation process of the predictive performance of the neural network model.

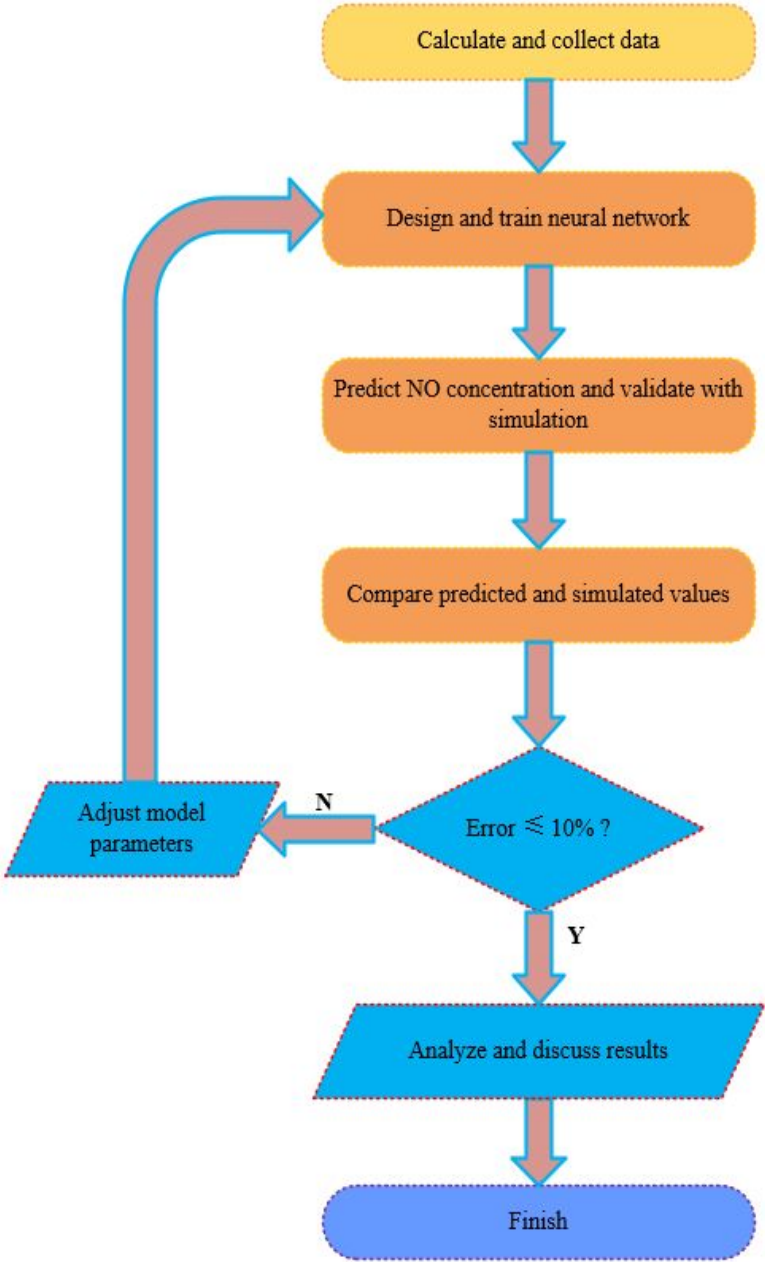


Fig. 13. Evaluation process of the predictive performance of the neural network model.

Operating parameters were generated within the ranges specified in **Table 1**. Simulations were conducted using COMSOL software to create a diverse and reliable dataset for model training. The data were then imported into MATLAB for training and validation of the neural network model. To ensure both accuracy and generalization, the dataset was split into training, validation, and test subsets. The input parameters for

the neural network model included temperature, pipe diameter, pipe length, inlet concentration, and inlet flow velocity. The NO concentration after denitrification served as the output parameter. Model weights were optimized using a backpropagation algorithm to minimize the error between predicted and simulated values. After training, the predictive performance of the model was evaluated using a test dataset excluded from the training set. The test set included various operating conditions, and the NO concentrations predicted by the neural network were compared with COMSOL simulation results to confirm prediction accuracy (**Table 5**). The relative errors between predicted and simulated values were required to remain below 10%. If the relative error exceeded this threshold, the model was refined through the modification of the network structure, expansion of the training dataset, or optimization of training parameters. Additionally, the model was re-trained and validated. After repeated iterations of adjustments and validation, once the relative error met the predetermined criteria, the neural network model was considered to have a high predictive accuracy. Consequently, the model can reliably predict the NO concentration after denitrification under different input conditions. This approach provides a basis for further investigation.

Table 5. Comparison of predicted values with simulated results under different conditions.

Temperature (°C)	Pipe diameter (mm)	Pipe length (mm)	Inlet concentration (mol/m ³)	Flow velocity (m/s)	Outlet concentration (mol/m ³)	
					Predicted	Simulated
117	50	957	0.02	3.62	0.01030	0.01031
143	50	1563	0.02	4.46	0.00240	0.00230
126	50	2456	0.02	3.45	0.00120	0.00124
133	50	2856	0.02	4.56	0.00083	0.00088
113	50	945	0.04	3.34	0.02250	0.02262
136	50	1459	0.04	4.66	0.01010	0.01012
128	50	2374	0.04	3.58	0.00330	0.00334
142	50	2785	0.04	4.74	0.00100	0.00110
113	80	867	0.02	3.23	0.01090	0.01109

(Table 5. Continued)

Temperature (°C)	Pipe diameter (mm)	Pipe length (mm)	Inlet concentration (mol/m ³)	Flow velocity (m/s)	Outlet concentration (mol/m ³)	
					Predicted	Simulated
132	80	1326	0.02	4.26	0.00530	0.00530
129	80	2572	0.02	3.45	0.00070	0.00073
137	80	2772	0.02	4.28	0.00047	0.00046
118	80	1075	0.04	4.52	0.02270	0.02266
140	80	1567	0.04	3.72	0.00440	0.00436
131	80	2549	0.04	4.69	0.00410	0.00448
133	80	2866	0.04	4.25	0.00190	0.00189

4. Optimization results

Comprehensive optimizations of temperature, flow velocity, and pipe length were conducted at a constant pipe diameter and inlet NO concentration. In these optimizations, the NO emission standard was set at 0.00167 mol/m³, and a genetic algorithm was utilized to minimize the overall operating cost. Owing to the strict penalty imposed for exceeding the emission standard, the NO concentration after denitrification was maintained below this limit.

4.1 Optimization results

A narrow pipe length range of 2100–3000 mm was selected. The specific ranges for temperature and flow velocity are shown in **Table 1**. Additionally, optimizations were performed independently for pipe diameters of 50 and 80 mm (**Table 6** and **Table 7**), respectively.

Table 6. Optimized parameters and corresponding costs for a pipe diameter of 50 mm.

Pipe Diameter (mm)	Inlet concentration (mol/m ³)	Optimization objective	Optimization results				
			Length (mm)	Temperature (°C)	Velocity (m/s)	<i>P</i> (CNY/h)	<i>P'</i> (CNY/kg)
50	0.02	Minimizing <i>P</i>	2100	128.9962	3.0115	11.0661	-
		Minimizing <i>P'</i>	2100	139.1558	4.8757	-	0.2611
	0.04	Minimizing <i>P</i>	2100	139.7202	3.2407	11.2358	-
		Minimizing <i>P'</i>	2100	148.4687	4.5680	-	0.2799

Table 7. Optimized parameters and corresponding costs for a pipe diameter of 80 mm.

Pipe Diameter (mm)	Inlet concentration (mol/m ³)	Optimization objective	Optimization results				
			Length (mm)	Temperature (°C)	Velocity (m/s)	<i>P</i> (CNY/h)	<i>P'</i> (CNY/kg)
80	0.02	Minimizing <i>P</i>	2100	127.8182	3.1341	27.8594	-
		Minimizing <i>P'</i>	2100	142.0124	4.9529	-	0.2534
	0.04	Minimizing <i>P</i>	2100	136.2247	3.0049	27.9679	-
		Minimizing <i>P'</i>	2100	145.8478	4.9301	-	0.2555

1
2
3
4
5
6
7
8
9
10
11
12
13
14
15
16
17
18
19
20
21
22
23
24
25
26
27
28
29
30
31
32
33
34
35
36
37
38
39
40
41
42
43
44
45
46
47
48
49
50
51
52
53
54
55
56
57
58
59
60

Table 6 shows the optimized parameters and corresponding costs for a pipe diameter of 50 mm. The data in the two left columns are fixed during the optimizations, while the third column shows the optimization objectives. The minimization analysis of total hourly cost (P) reveals that as the inlet NO concentration increases, the pipe length remains at the lower limit of the specified range. Moreover, the temperature increases from 128.9962°C to 139.7202°C, the flow velocity increases from 3.0115 to 3.2407 m/s, and the optimal P increases from 11.0661 to 11.2358 CNY/h. The minimization analysis of cost per unit mass (P') reveals that as the inlet NO concentration increases, the pipe length remains constant, while the temperature increases from 139.1558°C to 148.4687°C. Additionally, the flow velocity decreases from 4.8757 to 4.5680 m/s, and the optimal P' increases from 0.2611 to 0.2799 CNY/kg.

The optimization results for a pipe diameter of 80 mm are presented in **Table 7**. The minimization analysis of total hourly cost P indicates that as the inlet NO concentration increases, the pipe length remains at the lower limit of the specified range, while the temperature increases from 127.8182°C to 136.2247°C. Moreover, the flow velocity decreases from 3.1341 to 3.0049 m/s, and the optimal P increases from 27.8594 to 27.9679 CNY/h. The minimization analysis of P' indicates that with increasing inlet NO concentration, the pipe length remains constant, and the temperature increases from 142.0124°C to 145.8478°C. The flow velocity slightly changes, while optimal P' increases from 0.2534 to 0.2555 CNY/kg.

Notably, all optimized pipe lengths reach the lower limit of the specified range, indicating that this limit should be reduced.

4.2 Optimization results with adjusted ranges

In this section, the pipe length range was expanded from 800 to 3000 mm. With other conditions unchanged, optimizations were conducted, and the results are summarized in **Table 8** and **Table 9**.

Table 8. Optimized parameters and corresponding costs for a pipe diameter of 50 mm

(Pipe length range: 800 to 3000 mm).

Pipe Diameter (mm)	Inlet concentration (mol/m ³)	Optimization objective	Optimization results				
			Length (mm)	Temperature (°C)	Velocity (m/s)	P (CNY/h)	P' (CNY/kg)
50	0.02	Minimizing P	975.56	149.9949	3	5.6758	-
		Minimizing P'	1386.17	149.9592	4.3625	-	0.2029
	0.04	Minimizing P	1303.59	149.9793	3	7.3114	-
		Minimizing P'	1485.15	150	3.5120	-	0.2603

Table 9. Optimized parameters and corresponding costs for a pipe diameter of 80 mm

(Pipe length range: 800 to 3000 mm).

Pipe Diameter (mm)	Inlet concentration (mol/m ³)	Optimization objective	Optimization results				
			Length (mm)	Temperature (°C)	Velocity (m/s)	P (CNY/h)	P' (CNY/kg)
80	0.02	Minimizing P	944.51	150	3.0862	13.9148	-
		Minimizing P'	952.89	150	3.1600	-	0.1903
	0.04	Minimizing P	1358.25	149.9932	3.0625	19.0581	-
		Minimizing P'	1726.92	148.6192	4.8412	-	0.2193

For a pipe diameter of 50 mm, an increase in the inlet NO concentration from 0.02 to 0.04 mol/m³ results in several observable trends in the minimization analysis of P (**Table 8**). The pipe length increases from 975.56 to 1303.59 mm, the temperature slightly changes, the flow velocity remains at its lower limit, and the optimal P increases from 5.6758 to 7.3114 CNY/h. In the minimization analysis of P' , the increase in the inlet NO concentration causes the pipe length to increase from 1386.17 to 1485.15 mm. The temperature undergoes slight variations, the flow velocity decreases from 4.3625 to 3.5120 m/s, and the optimal P' increases from 0.2029 to 0.2603 CNY/kg.

For a pipe diameter of 80 mm, an increase in the inlet NO concentration from 0.02 to 0.04 mol/m³ leads to several notable trends in the minimization analysis of P (**Table 9**). The pipe length increases from 944.51 to

1358.25 mm, the temperature and flow velocity remain nearly constant, and the optimal P increases from 13.9148 to 19.0581 CNY/h. In the minimization analysis of P' , the increased inlet NO concentration leads to an increase in the pipe length from 952.89 to 1726.92 mm. Additionally, the temperature decreases from 150°C to 148.6192°C, the flow velocity increases from 3.1600 to 4.8412 m/s, and the optimal P' increases from 0.1903 to 0.2193 CNY/kg.

The optimization results with adjusted parameter ranges indicate improved operational efficiency, highlighting the vital role of selecting appropriate parameter ranges to optimize active coke-based NO removal.

4.3 Analysis of optimized costs

Under the third-row conditions in Table 9 (80 mm pipe diameter and 0.02 mol/m³ inlet concentration), the optimized cost per unit mass of processed flue gas was 0.1903 CNY/kg. A detailed analysis of the cost components is shown in Fig. 14.

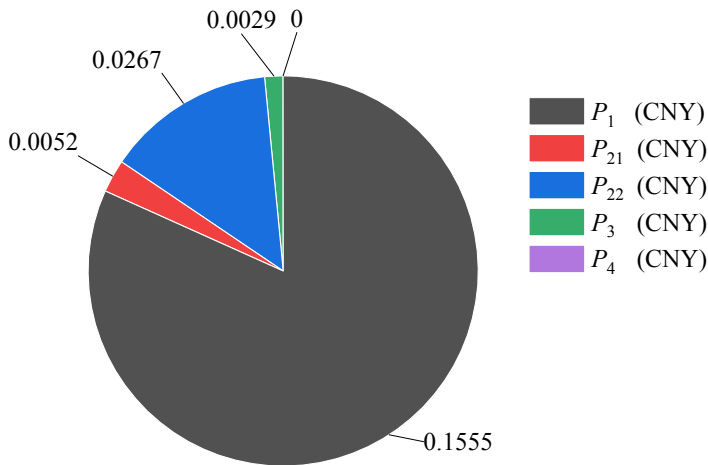


Fig. 14. Cost components under the third-row conditions in Table 9 ($P' = 0.1903$ CNY/kg).

The cost of processing one unit mass of flue gas comprises several components (Fig. 14). The cost of supplying active coke (P_1) is 0.1555 CNY, the heating cost of active coke (P_{21}) is 0.0052 CNY, the heating cost of flue gas (P_{22}) is 0.0267 CNY, and the operating cost of the fan (P_3) is 0.0029 CNY. Notably, the emission penalty (P_4) is 0 CNY, indicating full compliance with national emission standards.

5. Conclusion

This study numerically investigated active coke-based NO removal through COMSOL simulations. The effects of pipe diameter, temperature, pipe length, flow velocity, and inlet NO concentration on denitrification performance were analyzed. A neural network model was developed in MATLAB to predict the denitrification performance of active coke based on a large dataset generated from simulations. Moreover, key parameters, including temperature, flow velocity, and pipe length, were optimized using a genetic algorithm to enhance the denitrification efficiency and cost-effectiveness of the active coke-based NO removal system. The main conclusions are summarized as follows:

(1) As other parameters are held constant, the NO concentration in the outlet flue gas decreases with increasing temperature and pipe length but increases with higher inlet flow velocity and inlet NO concentration.

(2) The developed neural network model accurately predicts the NO removal performance of active coke and can be applied to further optimization tasks.

(3) he proposed approach—combining neural network prediction with genetic algorithm optimization—effectively identifies cost-efficient schemes for active coke-based NO removal. The optimized parameters significantly improve the operational cost-effectiveness and performance of the ACD system.

(4) As the NO concentration in the inlet flue gas increases, the optimized pipe length, temperature, and flow velocity vary. Consequently, both the total hourly cost and the cost per unit mass significantly increase. Notably, the cost of active coke accounts for the largest proportion of the total flue gas processing cost.

(5) The effectiveness of the proposed optimization method strongly depends on the defined parameter ranges. Setting appropriate parameter ranges significantly improves the efficiency of the optimization process.

Acknowledgments

This research was supported by the National Natural Science Foundation of China (No. 52106219).

References

- [1] Wang, W., Tian, S., Long, J., et al. (2022). Investigation and Evaluation of Flue Gas Pollutants Emission in Waste-to-Energy Plant with Flue Gas Recirculation. *Atmosphere*, 13(7), 1016.
- [2] Chang, J., Ma, X., Wang, X., Li, X. (2023). CPFD modeling of hydrodynamics, combustion and NO_x emissions in an industrial CFB boiler. *Particuology*, 81, 174-188.

1
2
3
4
5
6
7
8
9
10
11
12
13
14
15
16
17
18
19
20
21
22
23
24
25
26
27
28
29
30
31
32
33
34
35
36
37
38
39
40
41
42
43
44
45
46
47
48
49
50
51
52
53
54
55
56
57
58
59
60

[3] Zhang, J. X., Zhang, S., Cai, W., et al. (2013). The characterization of CrCe-doped on TiO₂-pillared clay nanocomposites for NO oxidation and the promotion effect of CeO_x. *Applied Surface Science*, 268, 535-540.

[4] Larki, I., Zahedi, A., Asadi, M., et al. (2023). Mitigation approaches and techniques for combustion power plants flue gas emissions: A comprehensive review. *Science of The Total Environment*, 903, Article 166108.

[5] Mukherjee, S., Kalra, G., Bhatla, S. C. (2025). Atmospheric nitrogen oxides (NO_x), hydrogen sulphide (H₂S) and carbon monoxide (CO): Boon or Bane for plant metabolism and development?. *Environmental Pollution*, Article 125676.

[6] Fenimore, C. P. (1971). Formation of nitric oxide in premixed hydrocarbon flames. *Symposium (International) on Combustion*, 13(1), 373-380.

[7] Hocking, M. B. (2012). *Modern chemical technology and emission control*. Springer Science & Business Media.

[8] Jin, G., Wang, M., Wang, S., et al., 2024. Co-combustion strategy of waste energetic materials with pine sawdust for efficient NO_x emissions reduction. *Journal of the Energy Institute*, 112, Article 101457.

[9] Cheng, X., Bi, X. T. (2014). A review of recent advances in selective catalytic NO_x reduction reactor technologies. *Particuology*, 16, 1-18.

[10] Wang, D., Li, S., Yang, S., et al. (2020). Current status and prospects of the application of industrial denitration technology. *Science & Technology in Chemical Industry*, 28(2), 77-82.

[11] Fu, Y., Zhang, Y., Li, G., et al. (2017). NO removal activity and surface characterization of activated carbon with oxidation modification. *Journal of the Energy Institute*, 90(5), 813-823.

[12] Wang, X., Cai, J., Chen, R., et al. (2025). Effect of different components in cement raw meal on carbothermal reduction of NO_x in flue gas: An experimental study. *Particuology*, 99, 23-33.

[13] Yang, J., Yuan, S., Shen, B., et al. (2020). Review on NO_x Removal with Non-thermal Plasma. *Science Technology and Engineering*, 20(15), 5917-5925.

[14] Bian, Z., Chen, Y., Zhi, Z., et al. (2023). Comparison of microbial community structures between oil and water phases in a low-permeability reservoir after water flooding. *Energy Reports*, 9, 1054-1061.

[15] Guan, X.J., Dong, D.T., Ma, P.J., et al. (2002). Research Progress in Production and Removal of Nitric

- 488 Oxides. Journal of Qingdao University of Technology, 23(4), 35–40.
- 489 [16] Wang, J.H. (2018). Application and comparison of SCR, SNCR and SNCR/SCR flue gas denitration
490 technology. Electric Power Technology and Environmental Protection, 34(5), 35–36.
- 491 [17] Wen, W., Wen, C., Wang, D., et al. (2024). A review on activated coke for removing flue gas pollutants
492 (SO₂, NO_x, Hg₀, and VOCs): Preparation, activation, modification, and engineering applications.
493 Journal of Environmental Chemical Engineering, 12(2), Article 111964.
- 494 [18] Yang, J.G., Wu, M.D., Gao, J., et al. (2025). Economic and carbon emission analysis of two typical
495 denitrification systems for sintering process in the iron and steel industry. Journal of Environmental
496 Sciences, 156, 79–90.
- 497 [19] Brozinčević, A., Grgas, D., Štefanac, T., et al. (2024). Cost Reduction in the Process of Biological
498 Denitrification by Choosing Traditional or Alternative Carbon Sources. Energies, 17(15), 3660.
- 499 [20] Yang, D. (2013). Application Status and Economic Analysis of Active Coke Flue Gas Desulfurization
500 Technology. Advanced Materials Research, 610, 1463–1468.
- 501 [21] Wu, Z., Li, D., Chen, H., Zhang, S., et al. (2021). Engineering application of desulfurization and
502 denitrification comprehensive purification technology for activated coke. Environmental Progress &
503 Sustainable Energy, 40, Article e13642.
- 504 [22] Liu, F. Q. (2018). A Low-Cost Activated Carbon Desulfurization and Denitrification Device.
505 CN206837782U.
- 506 [23] Chen, H. F., Feng, Z. H., Chen, H. W., et al. (2020). A Low-Cost Device for Activated Carbon
507 Desulfurization and Denitrification. CN210544344U.
- 508 [24] Tang, S. J., Lu, Q., Qu, Y. C., et al. (2019). Catalyst Volume Design in SCR Denitification System
509 Based on Genetic Algorithm Optimized BP Neural Network. Power Generation Technology, 40(3),
510 246–252.
- 511 [25] Meng, F. W., Xu, B., Lu, X. Y., et al. (2017). Application of Neural Network Predictive Control in SCR
512 Flue Gas Denitration System. Journal of Northeastern University (Natural Science), 38 (6), 778–782.
- 513 [26] Yang, T. T., Bai, Y., Lu, Y., et al. (2021). Study on Multi-objective Optimal Control of SCR
514 Denitrification System. Proc. Proceedings of the CSEE, 41(14), 4905–4911.
- 515 [27] Tang, C. J., Sun, J. F., Dong, L. (2020). Recent progress on elimination of NO_x from flue gas via SCR

1
2
3
4
5
6
7
8
9
10
11
12
13
14
15
16
17
18
19
20
21
22
23
24
25
26
27
28
29
30
31
32
33
34
35
36
37
38
39
40
41
42
43
44
45
46
47
48
49
50
51
52
53
54
55
56
57
58
59
60

technology under ultra-low temperatures ($< 150^{\circ}\text{C}$). CIESC Journal, 71(11), 4873–4884+5362.

[28] Dai, W. T. (2017). Study on adsorption characteristics of activated coke on SO_2 and numerical study on flow field of fixed bed reactor. Xi'an University of Architecture and Technology.

[29] Wen, Q. B. (2012). Preparation of Catalyst for Selective Catalytic Reduction of NO_x at Low Temperature and its Numerical Simulation. Hunan University.

[30] Long, R. Q., Yang, R. T. (2001). Fe-ZSM-5 for selective catalytic reduction of NO with NH_3 : a comparative study of different preparation techniques. Catalysis Letters, 74, 201–205.

[31] Wang, G., An, L. (2012). COMSOL Multiphysics Engineering Practice and Theoretical Simulation: Multiphysics Numerical Analysis Technology. Publishing House of Electronics Industry.

[32] Zhang, Q., Xu, S. S., Wang, Z. Q. (2004). Advancement and Engineering Application of Flue Gas Denitrification Technology by Using Selective Catalytic Reduction Method. Thermal Power Generation, 33(4), 1–6.

[33] Standardization Administration of the People's Republic of China. (2019). Pipe work components—Definition and selection of nominal size. Retrieved from http://www.weboos.cn:8083/assets/basicStandard/std_1538541.pdf. accessed October 20, 2024.

[34] Adelekan, D. S., Ohunakin, O. S., Paul, B. S. (2022). Artificial intelligence models for refrigeration, air conditioning and heat pump systems. Energy Reports, 8, 8451-8466.

[35] Abell, L. (2017). Neural Networks and Applications Using Matlab: Fit Data, Classify Patterns, Cluster Data and Time Series.

[36] Nguyen, D. V., Seo, M., Chen, Y., et al. (2025). Enhancing hydrogen sulfide control in urban sewer systems using machine learning models: Development of a new predictive simulation approach by using boosting algorithm. Journal of Hazardous Materials, 491, Article 137906.

[37] Chipperfield, A. J., Fleming, P. J. (1995, January). The MATLAB genetic algorithm toolbox. In IEE colloquium on applied control techniques using MATLAB (pp. 10-1). London UK: IEE.

[38] Purohit, G. N., Sherry, A. M., Saraswat, M. (2013). Optimization of function by using a new MATLAB based genetic algorithm procedure. Int. J. Comput. Appl, 61(15), 1–5.

[39] Dao, S. D., Abhary, K., Marian, R. (2017). An innovative framework for designing genetic algorithm structures. Expert systems with applications, 90, 196-208.

- 1
2
3 544 [40] Ribeiro Filho, J.L., Treleaven, P.C., Alippi, C. (1994). Genetic-algorithm programming environments.
4
5 545 Computer, 27(6), 28–43.
6
7 546 [41] Huang, T., Huang, J., Feng, M., et al. (2022). Optimization of the thickness of catalytic layer for HT-
8
9 547 PEMFCs based on genetic algorithm. Energy Reports, 8, 12905-12915.
10
11 548 [42] Farsi, M., Asemani, M., Rahimpour, M. R. (2014). Mathematical modeling and optimization of multi-
12
13 549 stage spherical reactor configurations for large scale dimethyl ether production. Fuel processing
14
15 550 technology, 126, 207-214.
16
17 551 [43] Al-Terkawi, L., Migliavacca, M. (2025). An automated parallel genetic algorithm with parametric
18
19 552 adaptation for distributed data analysis. Sci. Rep, 15(1), 10836.
20
21 553 [44] Lu, Y., Zhang, B., Cao, Y., et al. (2024). Exploring alkali-treated corn cob for high-rate removal of
22
23 554 NOX and SO2 from flue gas: Focus on carbon release capacity, removal performance, and comparison
24
25 555 with conventional carbon sources. Journal of Hazardous Materials, 478, 135613.
26
27 556 [45] Li, B. (2016). Research on Removal of Nitric Oxides from Flue Gas by Activated Coke Catalysis Action.
28
29 557 North China Electric Power University.
30
31
32
33
34
35
36
37
38
39
40
41
42
43
44
45
46
47
48
49
50
51
52
53
54
55
56
57
58
59
60

1
2
3
4
5
6
7
8
9
10
11
12
13
14
15
16
17
18
19
20
21
22
23
24
25
26
27
28
29
30
31
32
33
34
35
36
37
38
39
40
41
42
43
44
45
46
47
48
49
50
51
52
53
54
55
56
57
58
59
60

Highlights

- 1. NO removal using active coke particles was investigated via numerical simulations.
- 2. A neural network model was developed to predict denitrification efficiency.
- 3. Key operating parameters were optimized to enhance denitrification performance.
- 4. The optimization significantly reduced costs and maintained effective denitrification.

For Peer Review

Dear Edit-in-Chief,

Here within enclosed is our paper for consideration to be submitted on **SCIENCE PROCESS**. The work has not been published previously, is not under consideration for publication elsewhere, and is approved by all authors and host authorities. The further information about the paper is in the following:

The Title: **Multi-Parameter Analysis and Operating Cost Optimization for NO Removal using Active Coke**

The Authors: Wen Liu, Huawei Liu, Weiliang Cheng.

The authors claim that none of the material in the paper has been published or is under consideration for publication elsewhere.

Declarations of interest: none.

I am the corresponding author and my address and other information is as follows:

Address: *Key Laboratory of Power Station Energy Transfer Conversion and System of MOE, School of Energy Power and Mechanical Engineering, North China Electric Power University, Beijing 102206, China.*

E-mail: liuhw@ncepu.edu.cn

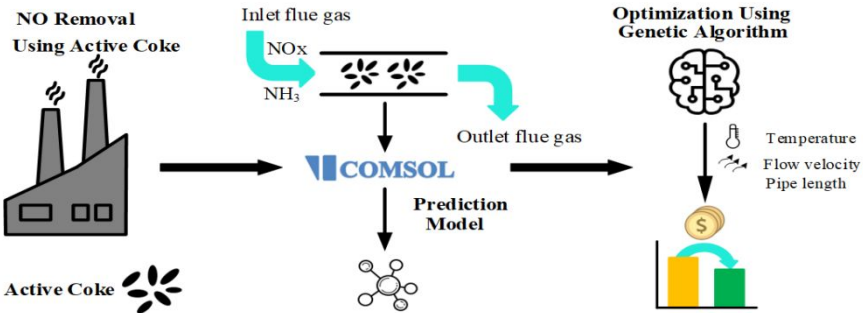
I hope this paper is suitable for **SCIENCE PROCESS**. We deeply appreciate your consideration of our manuscript, and we look forward to receiving comments from the reviewers. If you have any queries, please don't hesitate to contact me at the address below.

Thank you for your consideration.

Sincerely,

Dr. Huawei Liu

Graphical Abstract



For Peer Review

DECLARATION OF INTERESTS STATEMENT

The authors declare that they have no known competing financial interests or personal relationships that could have appeared to influence the work reported in this paper.

For Peer Review

1
2
3
4
5
6
7
8
9
10
11
12
13
14
15
16
17
18
19
20
21
22
23
24
25
26
27
28
29
30
31
32
33
34
35
36
37
38
39
40
41
42
43
44
45
46
47
48
49
50
51
52
53
54
55
56
57
58
59
60

Table 1. Simulation parameter ranges.

Temperature (°C)	Pipe diameter (mm)	Pipe length (mm)	Inlet concentration (mol/m ³)	Inlet flow velocity (m/s)
110~150	50 80	800~3000	0.02~0.04	3~5

For Peer Review

Table 1. Denitrification efficiency of active coke at different volumetric flow rates.

Volumetric flow rates (L/min)	Denitrification efficiency (%)	
	Experiment	Simulation
1	81.32%	76.10%
2	46.62%	47.14%
4	28.13%	26.27%

For Peer Review

1
2
3
4
5
6
7
8
9
10
11
12
13
14
15
16
17
18
19
20
21
22
23
24
25
26
27
28
29
30
31
32
33
34
35
36
37
38
39
40
41
42
43
44
45
46
47
48
49
50
51
52
53
54
55
56
57
58
59
60

Table 1. Effect of pipe diameter on the outlet NO concentration.

Temperature (°C)	Pipe diameter (mm)	Pipe length (mm)	Inlet concentration (mol/m ³)	Flow velocity (m/s)	Amount of flue gas processed per hour (m ³ /s)	Outlet concentration (mol/m ³)
120	50	1100	0.02	3	0.0059	0.007054
	80			3	0.0151	0.006972
	80			1.17	0.0059	0.000882

For Peer Review

Table 1. Effect of inlet NO concentration on the outlet NO concentration.

Temperature (°C)	Pipe diameter (mm)	Pipe length (mm)	Inlet concentration (mol/m ³)	Flow velocity (m/s)	Outlet concentration (mol/m ³)
120	50	1100	0.02	3	0.007054
			0.03		0.011205
			0.04		0.015524

For Peer Review

1
2
3
4
5
6
7
8
9
10
11
12
13
14
15
16
17
18
19
20
21
22
23
24
25
26
27
28
29
30
31
32
33
34
35
36
37
38
39
40
41
42
43
44
45
46
47
48
49
50
51
52
53
54
55
56
57
58
59
60

Table 1. Comparison of predicted values with simulated results under different conditions.

Temperature (°C)	Pipe diameter (mm)	Pipe length (mm)	Inlet concentration (mol/m ³)	Flow velocity (m/s)	Outlet concentration (mol/m ³)	
					Predicted	Simulated
117	50	957	0.02	3.62	0.01030	0.01031
143	50	1563	0.02	4.46	0.00240	0.00230
126	50	2456	0.02	3.45	0.00120	0.00124
133	50	2856	0.02	4.56	0.00083	0.00088
113	50	945	0.04	3.34	0.02250	0.02262
136	50	1459	0.04	4.66	0.01010	0.01012
128	50	2374	0.04	3.58	0.00330	0.00334
142	50	2785	0.04	4.74	0.00100	0.00110
113	80	867	0.02	3.23	0.01090	0.01109
132	80	1326	0.02	4.26	0.00530	0.00530
129	80	2572	0.02	3.45	0.00070	0.00073
137	80	2772	0.02	4.28	0.00047	0.00046
118	80	1075	0.04	4.52	0.02270	0.02266
140	80	1567	0.04	3.72	0.00440	0.00436
131	80	2549	0.04	4.69	0.00410	0.00448
133	80	2866	0.04	4.25	0.00190	0.00189

Table 1. Optimized parameters and corresponding costs for a pipe diameter of 50 mm.

Pipe Diameter (mm)	Inlet concentration (mol/m ³)	Optimization objective	Optimization results				
			Length (mm)	Temperature (°C)	Velocity (m/s)	P (CNY/h)	P' (CNY/kg)
50	0.02	Minimizing P	2100	128.9962	3.0115	11.0661	-
		Minimizing P'	2100	139.1558	4.8757	-	0.2611
	0.04	Minimizing P	2100	139.7202	3.2407	11.2358	-
		Minimizing P'	2100	148.4687	4.5680	-	0.2799

Table 1. Optimized parameters and corresponding costs for a pipe diameter of 80 mm.

Pipe Diameter (mm)	Inlet concentration (mol/m ³)	Optimization objective	Optimization results				
			Length (mm)	Temperature (°C)	Velocity (m/s)	<i>P</i> (CNY/h)	<i>P'</i> (CNY/kg)
80	0.02	Minimizing <i>P</i>	2100	127.8182	3.1341	27.8594	-
		Minimizing <i>P'</i>	2100	142.0124	4.9529	-	0.2534
	0.04	Minimizing <i>P</i>	2100	136.2247	3.0049	27.9679	-
		Minimizing <i>P'</i>	2100	145.8478	4.9301	-	0.2555

Table 1. Optimized parameters and corresponding costs for a pipe diameter of 50 mm

(Pipe length range: 800 to 3000 mm).

Pipe Diameter (mm)	Inlet concentration (mol/m ³)	Optimization objective	Optimization results				
			Length (mm)	Temperature (°C)	Velocity (m/s)	P (CNY/h)	P' (CNY/kg)
50	0.02	Minimizing P	975.56	149.9949	3	5.6758	-
		Minimizing P'	1386.17	149.9592	4.3625	-	0.2029
	0.04	Minimizing P	1303.59	149.9793	3	7.3114	-
		Minimizing P'	1485.15	150	3.5120	-	0.2603

Table 1. Optimized parameters and corresponding costs for a pipe diameter of 80 mm
(Pipe length range: 800 to 3000 mm).

Pipe Diameter (mm)	Inlet concentration (mol/m ³)	Optimization objective	Optimization results				
			Length (mm)	Temperature (°C)	Velocity (m/s)	<i>P</i> (CNY/h)	<i>P'</i> (CNY/kg)
80	0.02	Minimizing <i>P</i>	944.51	150	3.0862	13.9148	-
		Minimizing <i>P'</i>	952.89	150	3.1600	-	0.1903
	0.04	Minimizing <i>P</i>	1358.25	149.9932	3.0625	19.0581	-
		Minimizing <i>P'</i>	1726.92	148.6192	4.8412	-	0.2193

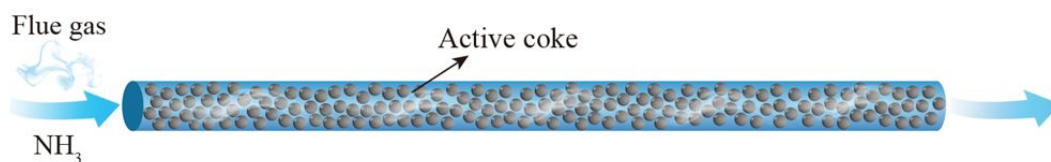


Fig. 1. Schematic of the denitrification pipe.

For Peer Review

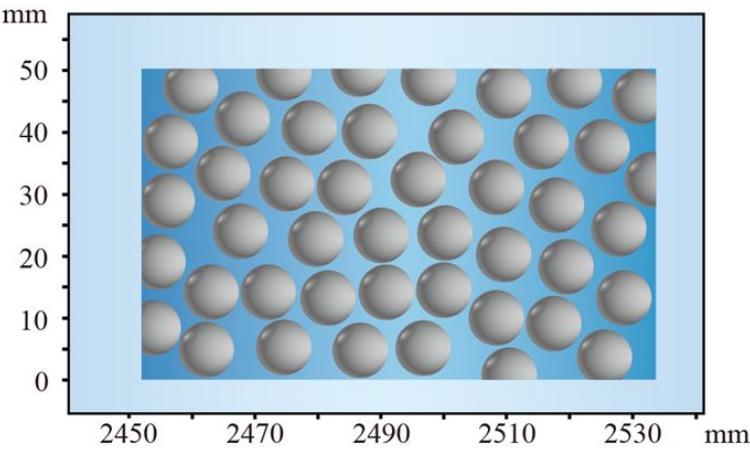


Fig. 1. Schematic of the randomly distributed active coke bed.

For Peer Review

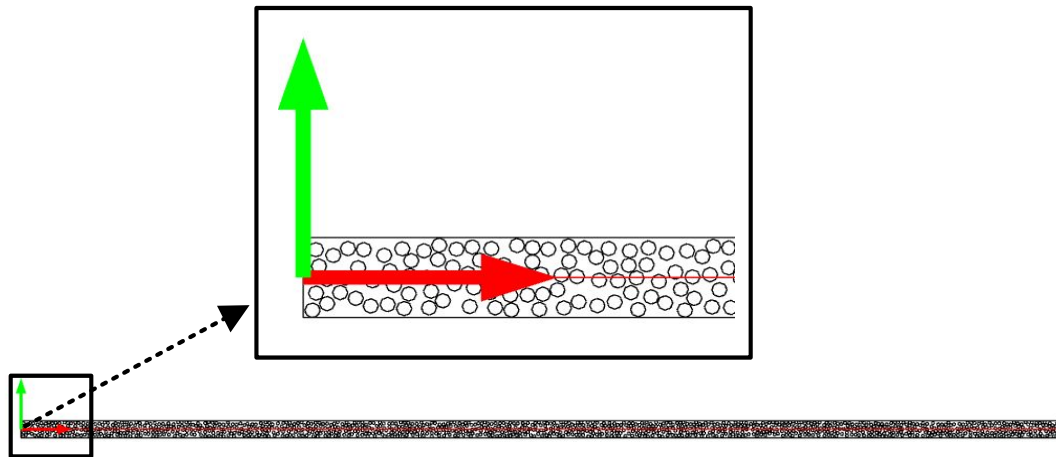


Fig. 1. Schematic of the centerline path.

For Peer Review

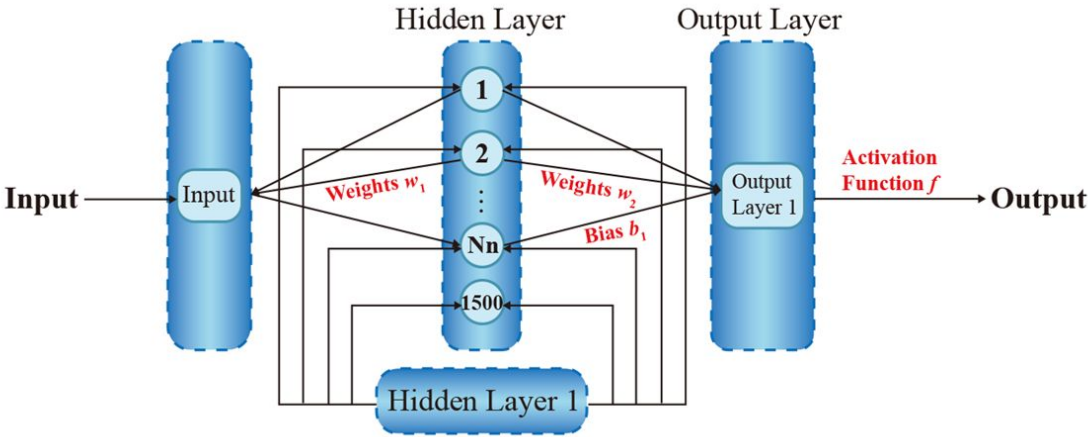


Fig. 1. Schematic of the neural network model.

For Peer Review

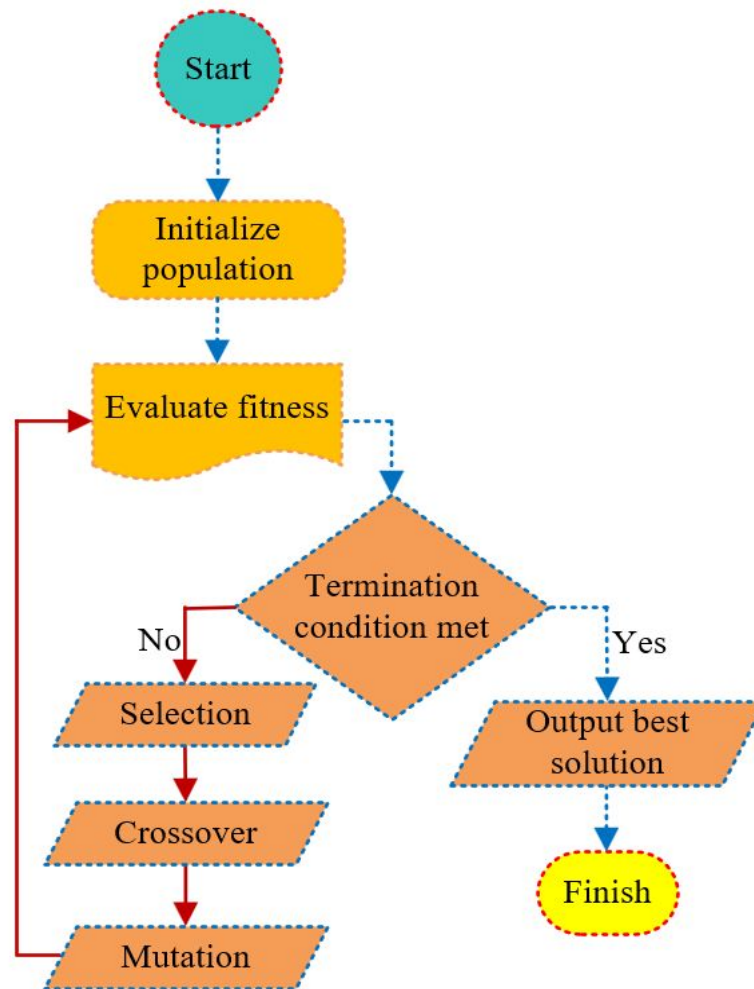


Fig. 1. Overview of the genetic algorithm optimization process.

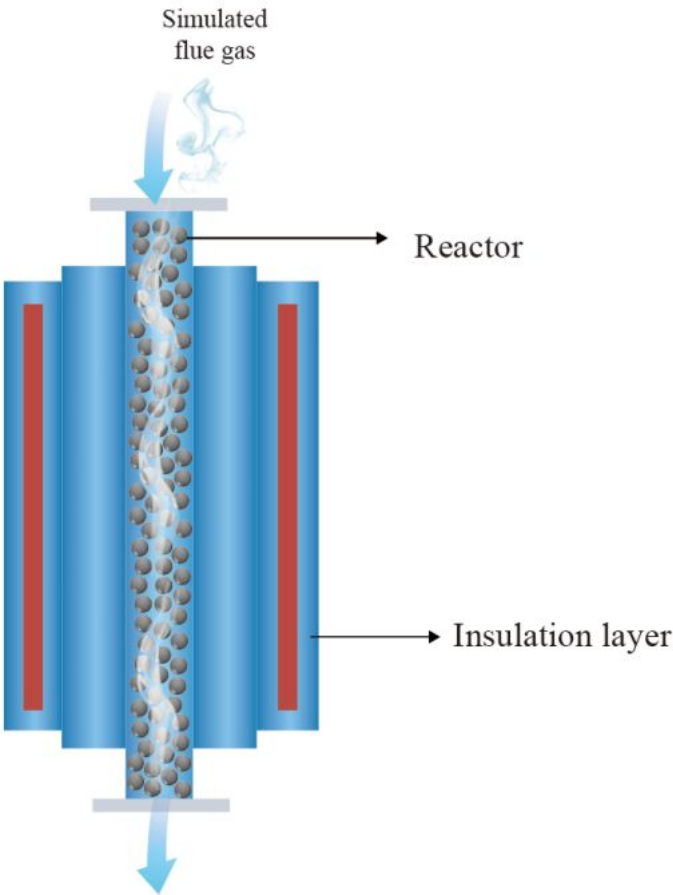


Fig. 1. Schematic of the experimental setup [45].

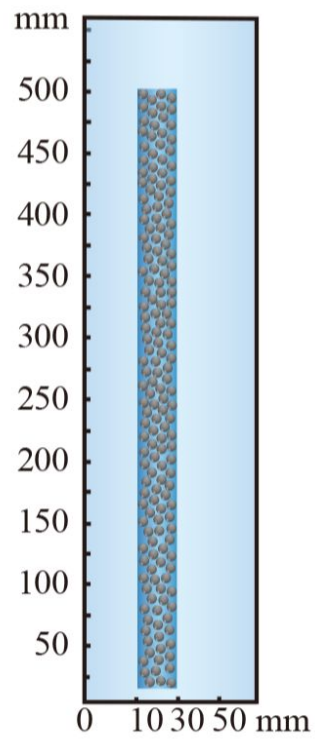


Fig. 1. Geometric model of the fixed-bed reactor.

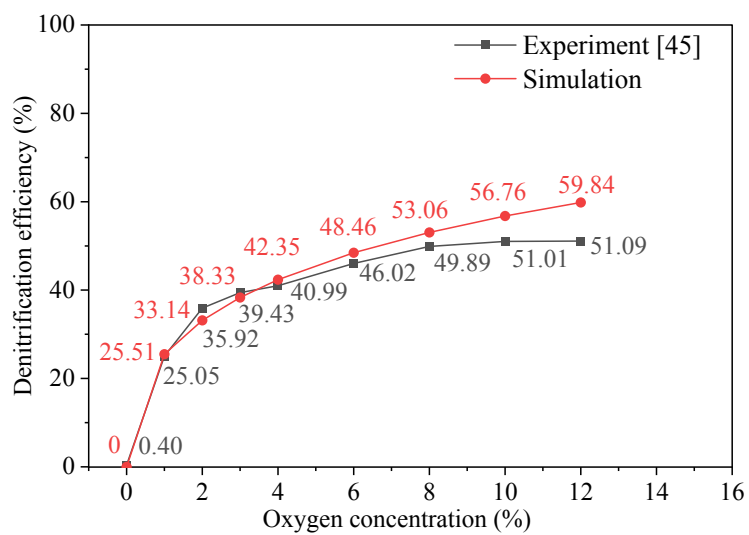


Fig. 1. Denitrification efficiency of active coke at different oxygen concentrations.

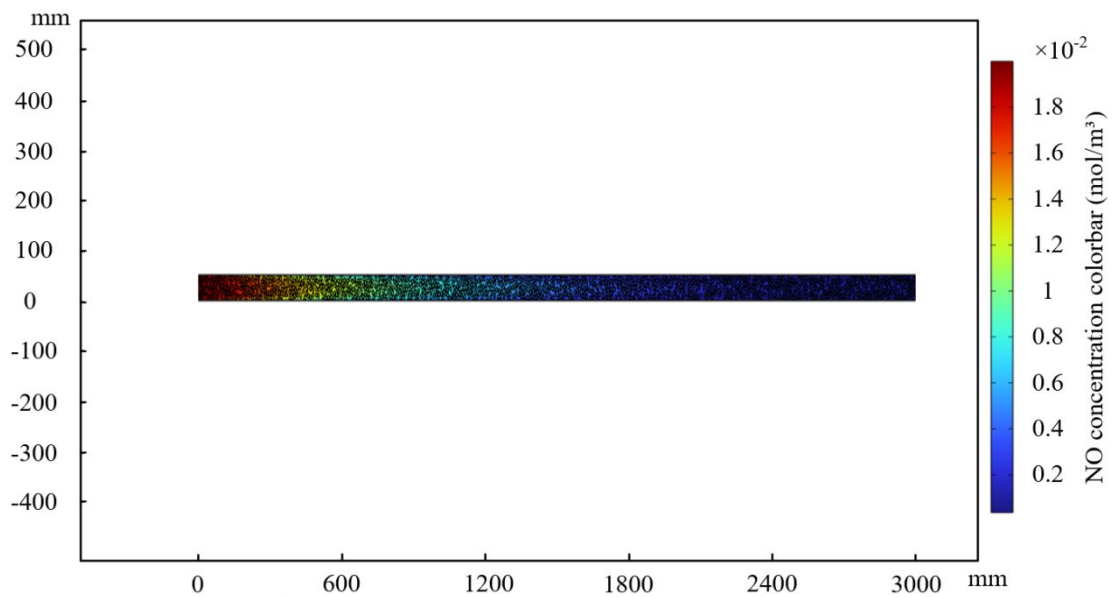


Fig. 1. Simulated distribution of NO concentration.

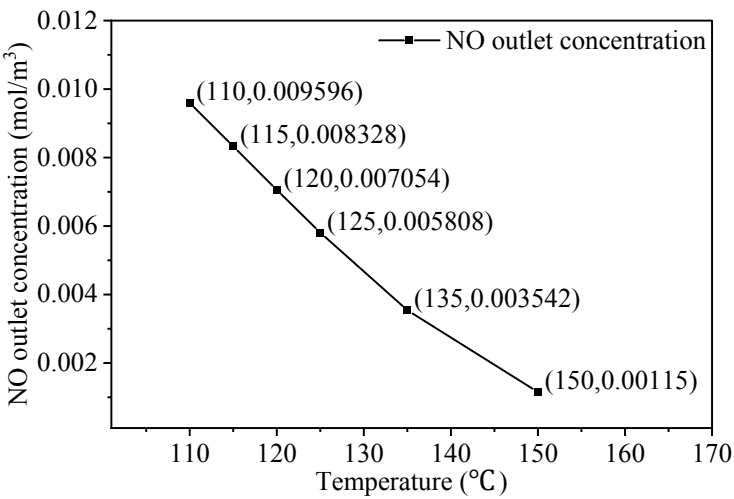


Fig. 1. Effect of temperature on the outlet NO concentration.

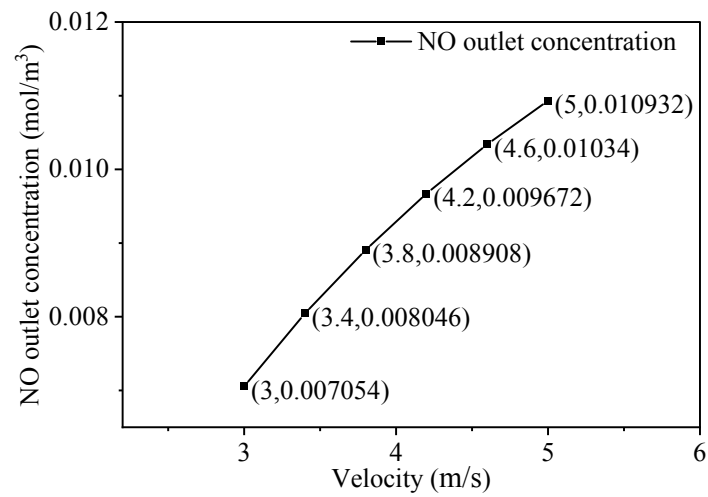


Fig. 1. Effect of flow velocity on the outlet NO concentration.

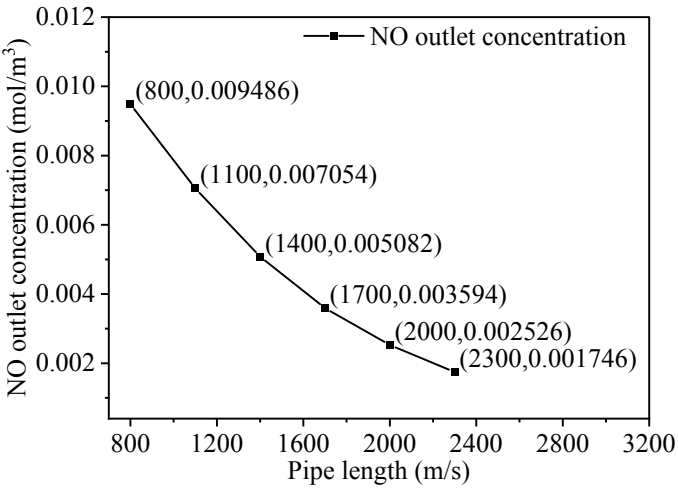


Fig. 1. Effect of pipe length on the outlet NO concentration.

For Peer Review

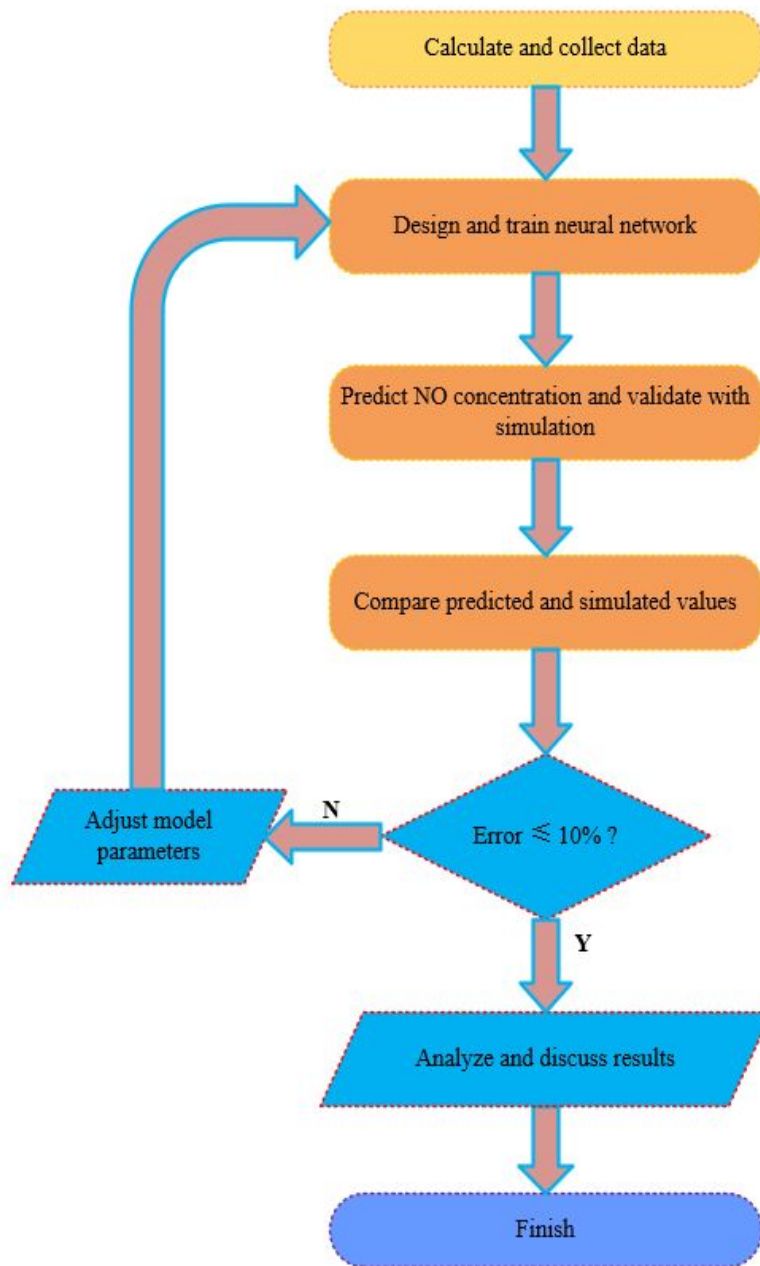


Fig. 1. Evaluation process of the predictive performance of the neural network model.

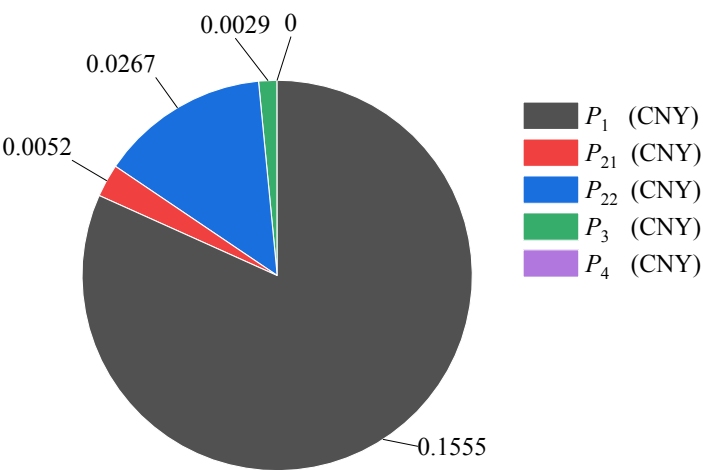


Fig. 1. Cost components under the third-row conditions in **Table 9** ($P' = 0.1903$ CNY/kg).

For Peer Review